

A TCM OFDM Software Transceiver

Ping-han Chiang, Ying-tzu Huang, Tsai-wen Chen, I-hsueh Lin, and Kwang-cheng Chen

Department of Electrical Engineering

National Taiwan University

Abstract — Orthogonal Frequency Division Multiplexing (OFDM), a multicarrier technique, is capable of coping with highly dispersive channels. In this paper, we adopt advanced Trellis Coded Modulation (TCM)-OFDM, instead of Convolutional Code (CC)-OFDM adopted by HIPERLAN/2 and IEEE 802.11a, to enhance the SNR requirement. A sophisticated OFDM transceiver is designed, including synchronizers in every aspect and the data-aided (DA) equalizer. We focus on the design and simulation of the high-speed OFDM system suitable for Wireless Local Area Network (WLAN) applications with the consideration of software radio implementation.

I. Introduction

OFDM is a promising technique that is able to cope with multipath channels, especially high speed wireless data communications. An OFDM system divides the available spectrum into several subchannels. The frequency responses of the subchannels are overlapping and orthogonal to each other, hence is named OFDM. When the subchannels are narrowband, they experience almost flat fading, and equalization is relatively simple. In addition, we further pioneerly adopt TCM, a breakthrough of combining modulation and coding by Gottfried Ungerboeck, to enhance link performance than state-of-the-art standard, such as IEEE 802.11a and ETSI HIPERLAN/2.

One improvement that distinguishes OFDM from ordinary FDM systems is the use of Discrete Fourier Transform (DFT)[1], which can be executed more quickly by Fast Fourier Transform (FFT) algorithm instead of oscillators to send the signals to high frequencies. Practical application of the OFDM system lies in the use of the cyclic prefix (CP)[2]. Traditionally, a

preceding guard interval (GI) can help reduce the intersymbol interference (ISI). However, to prevent the received signals from intercarrier interference (ICI), barely a GI is not enough. To maintain the orthogonality required to avoid ICI, the CP, which is a copy of the last part of the OFDM symbol, is introduced. The use of CP not only makes the transmitted signals periodic, but also reduces ISI and ICI in a constructive way.

Owing to the irreducible error floor in an uncoded OFDM system[3], the adoption of coding is therefore inevitable. According to the comparison made in [3], a Turbo-coded OFDM in spite of tremendous coding delay works the best among all the coding schemes, while it is also the most complicated one in algorithm and implementation. The TCM-OFDM system has the next best performance and is better than CC-OFDM adopted by HIPERLAN/2 and IEEE 802.11a with near complexity. Consequently, TCM-OFDM strikes the best compromise between performance and complexity.

II. Principle

Compared with regular single carrier systems, the complexity of equalization in an OFDM system does not grow exponentially with higher data rates. However, constructing OFDM systems is not simple owing to its high sensitivity to synchronization errors. Since orthogonality maintains only when the transmitter and receiver use exactly the same frequencies, frequency synchronization is thus critical to the performance of an OFDM system. Besides, timing offsets lead to unsatisfied performance in interpolation-type channel estimation[4], which affects the equalization simultaneously. Therefore, how to develop effective synchronization algorithms of satisfactory performance and

complexity has been an important issue.

Due to the inevitable adverse effects in the wireless environment, the transmitted signal is bound to be distorted under such channels. Therefore, to acquire the original desired signals, proper procedures must be taken, such as channel estimation, a characteristic way in coherent detection. Although differential detection needs no channel estimation in contrast to coherent detection, it has several drawbacks: the relatively poor performance, smaller tolerance of delay spread[5], and the difficulty in handling amplitude-modulated systems. Therefore, coherent detection is adopted in our design. We use DA interpolation-type channel estimation, which uses only the pilot subcarriers to acquire the sampled channel frequency response. To compensate the channel effects by zero forcing, simply multiply the signal by the reciprocal of the interpolated channel frequency response.

In the design of an OFDM receiver, at least three synchronization problems must be considered. The first is the frame timing synchronization problem, which can be solved by a careful design of the preamble. The second problem is frequency synchronization, which can be estimated and then compensated by exploiting information contained in the received preambles, pilot subcarriers, guard band, and CP. The last problem is about symbol timing and sample clock synchronization, which can be estimated by using pilot subcarriers and CP.

III. System Model

The block diagram of our design is shown in Fig. 1. The OFDM baseband signal of IFFT output using N subcarriers is[6]

$$x_n(j) = \frac{1}{N} \sum_{k=0}^{N-1} X_k(j) e^{j2pk_n} \quad (1)$$

where $X_k(j)$ is the modulated complex data of the k -th subcarriers in the j -th OFDM symbol, and n is the sample time. The transmitted OFDM symbol with CP is

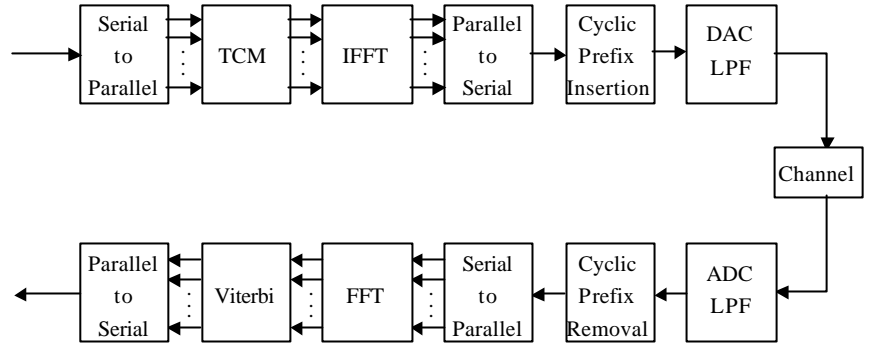


Fig. 1. The Block Diagram of OFDM

$$s_n(j) = \sum_{n=-G}^{N-1} x_n(j) \quad (2)$$

where G is the length of guard interval and the received n -th sample in the j -th OFDM symbol is[6]

$$y_n(j) = \frac{1}{N} \sum_{k=0}^{N-1} X_k(j) e^{j2p \frac{kn}{N}} H_k \cdot e^{j \left\{ 2pk \frac{T_d}{T_u} + 2pk \frac{\Delta t(j)}{T_u} + f_0 + 2p\Delta f T_{sym} \right\}} + \tilde{n}(jT_{sym} + nT_s) \quad (3)$$

where H_k is the channel frequency response at the k -th subcarrier, and T_d , $\mathbf{D}(j)$, \mathbf{f}_0 , and \mathbf{Df} are symbol timing offset, sample timing offset, phase offset, and frequency offset in the j -th OFDM symbol, respectively. T_u , T_s , and T_{sym} are the useful data duration, sample interval and the OFDM symbol duration, respectively. The FFT output for the k -th subcarriers in the j -th OFDM symbol is

$$Y_k(j) = X_k(j) H_k e^{j \left\{ 2pk \frac{T_d}{T_u} + 2pk \frac{\Delta t(j)}{T_u} + f_0 + 2p\Delta f T_{sym} \right\}} + I_k + N_k \quad (4)$$

where I_k is ICI from carrier frequency offset and N_k is noise for the k -th subcarrier. Thus the phase rotation at the k -th subcarrier of the j -th OFDM symbol from synchronization error is[6]

$$\mathbf{f}_k(j) = 2p_k \frac{T_d + \Delta t(j)}{T_u} + \mathbf{f}_0 + 2p\Delta f T_{sym} \quad (5)$$

IV. Design

4-1 Parameters

The parameters set in our system are listed

in Table 1. Since a radix-4 FFT is the least complex and the most efficient one in algorithm, we choose the number of FFT points as 64 here. The CP interval is assumed 1/4 long as the useful data duration. In this design, the accuracy of the carrier center frequency is within ± 62.5 ppm at 5GHz. Therefore, the range is set ± 50 ppm here to be on the safe side. Besides, The first subcarrier, namely the dc term, is set zero in order to facilitate the ADC/DAC. The outer subcarriers are set null to serve as the guard band in using a filter. The pilots are allocated at $+8^{\text{th}}$, -8^{th} , $+24^{\text{th}}$, and -24^{th} , respectively.

Table 1. System Parameters

Data rate	12Mbps
Modulation	QPSK
Coding	1/2 TCM
FFT point	64
Sample rate	20Msample/sec
Sample interval	0.05 μ s
OFDM Symbol Interval	4 μ s
Useful Data Duration	3.2 μ s
CP period	0.8 μ s
Data subcarriers	48
Subcarrier spacing	0.3125MHz
Pilot subcarrier	4
Pilot spacing	4.375MHz
Carrier center frequency	5GHz (Accuracy ± 50 ppm)
Occupied bandwidth	16.6MHz

4-2 Frame Timing and Carrier Frequency Synchronization

We adopt the Minimum Mean Square Error (MMSE) algorithm for frame timing in our system because of its performance advantage over Maximum Correlation (MC) algorithm and lower complexity than Maximum Likelihood (ML) algorithm[7]. Since our system is designed for burst-mode or packet-type transmission, certain form of power detecting wake-up

algorithm must be implemented. A long preamble can get a more accurate frequency offset estimate but the lock-in range is comparatively small. On the contrary, a shorter preamble can get a larger acquisition range, but accuracy is not as good. To meet the requirement of our system, we use short preambles first, which are used for coarse frequency synchronization, followed by long preambles, which are for frame timing and fine frequency synchronization, to get the best performance.

The structure of the preambles in our system is shown in Fig. 2. The first 32 samples are for wake-up use. Then, two identical 16 samples are used as short preambles, specified in IEEE 802.11a[8], to do coarse and wide range frequency offset estimation. Afterwards, we use 144 samples as long preambles to do fine frequency offset estimation and accurate frame timing estimation. The long preambles, specified in IEEE 802.11a[8], contain two identical 64-sample OFDM symbols. The usage of the 8-sample inverse cyclic prefix in the front of the long preambles and inverse cyclic postfix at the end of the long preambles will be discussed shortly.

The MMSE frame timing and carrier frequency synchronization algorithm is stated as follows. The received power sum and the complex correlation inside a frame of D_s received samples are[7]

$$P_k = \sum_{m=k}^{k+D_s-1} |y_m|^2 \quad (6)$$

$$S_k = \sum_{m=k}^{k+D_s-1} y_m^* y_{m+D_s} \quad (7)$$

In our system, $D_s=64$ for long preambles and $D_s=16$ for short preambles. The receiver continuously monitors the power sum in the receiving window, once the energy reaches a

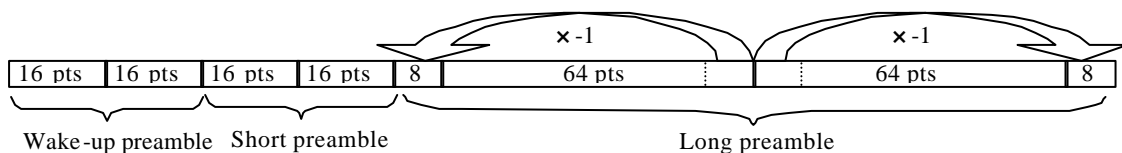


Fig. 2. Structure of data frame preambles

threshold value obtained by simulation, the receiver is waked up to perform frame synchronization algorithm. With MMSE criterion, the frame starting position is indicated as the metric $M_k = 2|S_k| - P_k - P_{k+D_s}$ reaches its maximum value. That is, the first sample of the two identical OFDM symbols in the preambles should be at $\hat{K} = \arg \max_k M_k$. In the process of finding the starting position, we store the maximum amplitude of M , the corresponding correlation S and the counter value[9]. If the incoming amplitude of M is larger than the stored maximum amplitude of M , the new values are updated and the counter value is reset. When the searching range the counter records reaches certain optimal value obtained by simulation, we take the stored maximum as the desired value. After the frame starting position \hat{K} is found, we can use it to estimate the normalized frequency offset \mathbf{x} by the following equation

$$\hat{\mathbf{x}} = \frac{D}{2pD_s} \text{angle}(S_{\hat{k}}) \quad (8)$$

where D is the length of an IFFT/FFT window in the data frame, i.e. $D=64$ in our system. \mathbf{x} is defined as the frequency offset Δf divided by OFDM subcarrier frequency spacing Δf_{sub} , i.e.

$$\mathbf{x} = \frac{\Delta f}{\Delta f_{sub}}$$

Thus we can get the accurate frame timing and fine frequency offset estimation. The expectation of power sum P , absolute value of complex correlation S , and metrics M in the interval of receiving long preamble are illustrated in Fig. 3.

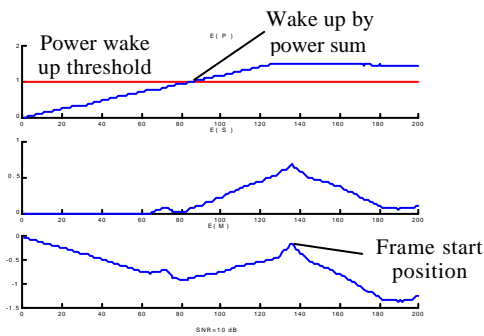


Fig.3 The metrics of frame synchronizartion

We can see that apart from $\hat{\mathbf{x}}$, any $\mathbf{x} = \hat{\mathbf{x}} + n \frac{D}{D_s}$, with $n \in Z$, is a possible normalized frequency offset estimate. Hence the normalized frequency offset must be confined in a range smaller than $\frac{D}{D_s}$ before we do the fine frequency offset estimation. Since a short preamble has smaller D_s , it can find frequency offset in a larger range.

The 8-sample inverse cyclic prefix and inverse cyclic postfix mentioned above are constructed to improve timing estimation accuracy. As the correlation window aligns with the two identical OFDM symbols in the preambles, i.e. at the frame starting position, the metric M reaches its maximum value. In order to avoid possible ambiguity, M is expected to decrease as quickly as possible when the window moves slightly away from the frame starting position. Consider the situation that the receiving window is one sample before the aligned position, that is, $k = \hat{k} - 1$. Since the sample just before the identical OFDM symbols in our long preamble is the inverse of the last sample in the OFDM symbol, the S_{k-1} in our design with the inverse cyclic prefix and inverse cyclic postfix will be smaller than the S_{k-1} with the ordinary cyclic prefix, while P_{k-1} remains the same. This will make the metrics M using such preamble change more sharply than those using conventional two identical symbol preambles. The improvement of such design is shown in Fig. 4.

Besides, when coarse frequency synchronization is working, we store necessary information in the buffer beforehand for the following frame timing and fine frequency synchronization to compute the summation recursively and reduce the complexity of track-back. After getting the coarse frequency offset estimation, we compensate the correlation values S of the incoming samples and the stored values by multiplying with $e^{-j2p\mathbf{x}}$ inferred from Eq.(7).

4-3 Symbol Timing Synchronization

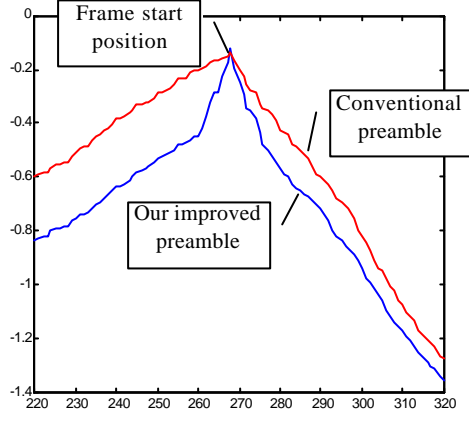


Fig.4 Expectation of M near frame start position

The pilots, originally used for channel estimation, simultaneously carry some information about timing. Besides the pilots, the CP of each transmitted OFDM symbol[10] with ML algorithm can also help in the symbol timing synchronization. The metrics from CP and pilot are

$$\Lambda_k^{cp} = \left| \sum_{n=k}^{k+L-1} y_n^* y_{n+D} \right| - \frac{\mathbf{r}}{2} \sum_{n=k}^{k+L-1} |y_n|^2 + |y_{n+D}|^2 \quad (9)$$

$$\Lambda_k^p = (1 + \mathbf{r}) \left| \sum_{n=k}^{k+D-1} y_n m_{n-k} \right| - \mathbf{r} \left| \sum_{n=k}^{k+L-1} (y_n + y_{n+D})^* m_{n-k} \right| \quad (10)$$

where L is the length of CP, m_k is the OFDM symbol containing purely pilots in the time domain, and fixed $\mathbf{r} = \frac{SNR}{SNR+1}$ is determined

by simulation to circumvent the SNR estimation. The OFDM symbol starting position is indicated as the joint metric $\Lambda_k = \mathbf{r}\Lambda_k^{cp} + (1-\mathbf{r})\Lambda_k^p$ reaches its maximum value. The expectation of Λ^p , Λ^{cp} and Λ is illustrated in Fig. 5. The Λ^p term increases the sharpness of Λ , hence the accuracy of the symbol timing estimation. The computing complexity can be reduced by calculating and comparing the Λ of only a few points around the 80th point. The beginning of the next symbol is thus set at the point of the maximum Λ . Such method can surely improve the computation efficiency significantly. Besides the integer sample offset of symbol timing synchronization error, there is the fractional sample offset of sample clock synchronization error. That the phase rotation of sample timing offset is negligible can be seen from Eq.(5). Therefore, the

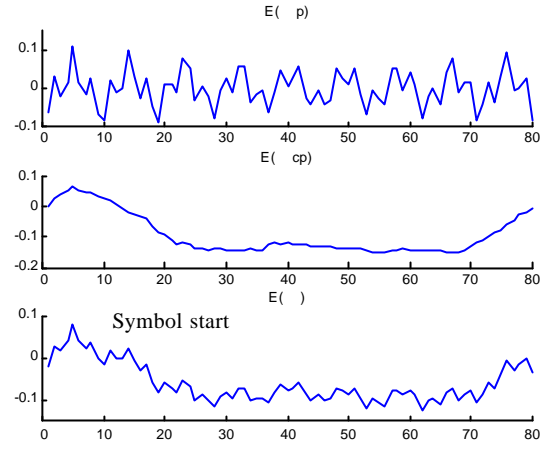


Fig.5 Symbol Timing Synchronization

sample clock synchronization is excluded here.

4-4 Equalization

In our design, channel estimation is achieved by the known pilots, since the decision-directed approach is not applicable in fast fading channels and is vulnerable to error propagation[11]. Therefore, interpolation is needed. The optimal interpolation filter is based on MMSE; however, due to significant computation complexity, a suboptimal approach based on Least Square (LS) and DFT that is not sensitive to the channel statistics[11] is adopted instead. As mentioned above, the use of FFT in place of DFT also helps reduce the time needed to complete the channel estimation. Firstly, the pilots are extracted and compared with the receiver-known ones, while the polarity of the previously known pilots depends on the cyclic extension of the 127 elements sequence, defined in IEEE 802.11a[8], and each of the elements is used for an OFDM symbol. In other words, the extracted pilots are divided by the known pilots to get a first estimate of the channel. Since the pilot pattern in our design is 1 or -1, we can use multiplication rather than division to ease the computing load. The four pilots are allocated uniformly along the 64 subcarriers, so we send the results through 4-point IFFT to the time domain. Afterwards, the outputs of the 4-point IFFT along with phase rotation and padded zeros, which are for interpolation use in the frequency domain, are sent to the 64-point FFT. The equalization coefficient is then acquired and equalization is done by multiplying the signal by its reciprocal.

4-5 TCM and Interleaving

We choose the generator polynomial of TCM with the popular convolutional encoder, used by Global System of Mobile Communication (GSM), as $(23,33)_8$ [12]. The coding rate, constraint length, and the number of states are $1/2$, 5, and 16, respectively. The mapper of Quadratic Phase Shift Keying (QPSK) is generated by set-partitioning, not conventional Gray mapping. The soft-decision Viterbi decoder is implemented without track-back steps to reduce complexity[13]. Although the decode length should be determined by simulation, it is taken as the number of data subcarriers for its suitability in our OFDM system. In addition, interleaving is used to overcome burst errors due to deep fading. Because the subchannel gains of OFDM system are the continuous channel frequency responses, the adjacent subchannels experience similar fading. To avoid the poor performance around the notches in frequency dispersive channels the Maximum Likelihood Sequential Estimation (MLSE) algorithm, namely Viterbi algorithm, may suffer, the periodic interleaving, which maps consecutive coded symbols apart from each other, is used to improve the performance [14].

V. Simulations

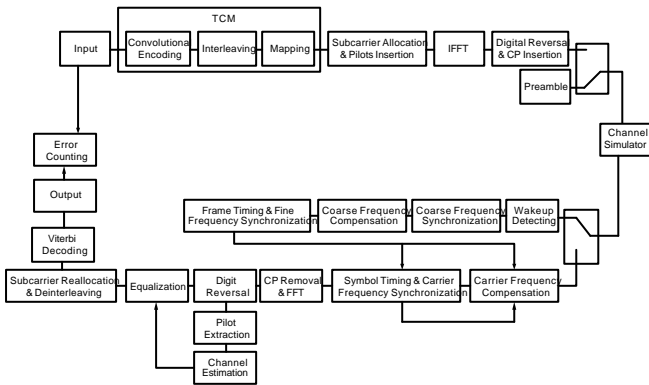


Fig. 6. The Overall Block Diagram

The overall block diagram of our design is shown in Fig.6. The three types of channels taken in our simulation are listed in Table 2 [15]. Because the influence of Doppler shift is comparatively small in portable applications, it is not included in the simulation. The uniform random frequency offset is set within ± 1.5

subcarriers spacing, while the uniform random phase offset is set between $\pm\pi$. The power gain of the channel is assumed one here.

Table 2. Power Profile of Simulating Channels

Type	Power Profile(dB)
AWGN	N/A
Rician	0,-5,-11,-17,-22,-28
Rayleigh	

The relationship of BER v.s. SNR is as plotted in Fig. 7. As the simulation results justify, the performance of our system is satisfactory as expected.

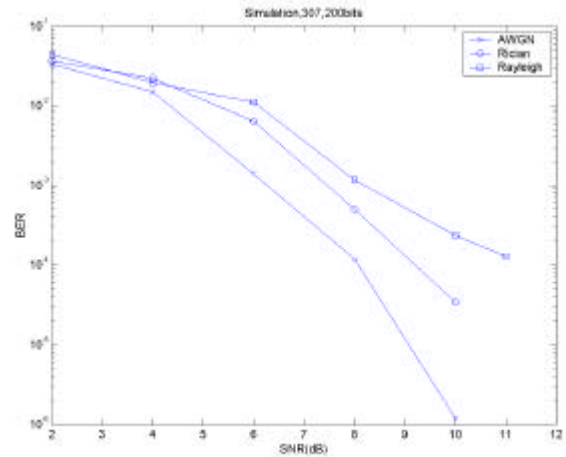


Fig. 7. The Simulation Results

VI. Conclusion

OFDM is a recently-emphasized technique. Because it enjoys many advantages suitable for the high-speed networks, it is regarded as the best approach to transmit data on the high-speed networks. Owing to its transmission with overlapping orthogonal signals in parallel, it can save the bandwidth in an efficient way. Furthermore, the complexity of the OFDM system does not grow exponentially as the bit rate increases. Therefore, it surely has considerable potential in practical applications. As our simulation results prove, under carefully-chosen algorithms, a TCM-OFDM system can perform quite well over 5 GHz. Not only the multipath problem, but also the frequency offset and the timing offset difficulties can be solved simultaneously. The distortion of channel effects can also be compensated by relatively simple

equalization scheme. Therefore, the future development on software environment, such as DSP, is promising. By exploiting the fixed-point architecture and the code optimization of a fixed-point DSP, the complexity of algorithms and computation can be eased. In conclusion, the future development of such a system is worth anticipating.

VII. Acknowledgement

The authors wish to express their grateful acknowledgement to Prof. Chen Kwang-cheng for his instruction in this paper. Furthermore, the authors are thankful for Liao Yi-ching, Liu Pei-chun, Chiu Wei-chen, and Chou Chia-tai for the fruitful discussions.

VIII. References

- <1>Weinstein, S. B., "Data Transmission by Frequency-Division Multiplexing Using the Discrete Fourier Transform", *IEEE Transactions on Communication Technology*, vol. com-19, No. 5, pp.628-634, Oct. 1971.
- <2>Bingham, J. A. C., "Multicarrier Modulation for Data Transmission: An Idea Whose Time Has Come", *IEEE Communications Magazine*, pp. 5-14, May 1990.
- <3>W.A.C. Fernando, R.M.A.P. Rajetheva, "Performance of Coded OFDM with Higher Modulation Schemes", ICCT 1998, Oct. 22-24, 1998
- <4>Yang, B., Letaief, K. B., Cheng, R. S. and Cao Z., "Burst Frame Synchronization for OFDM Transmission in Multipath Fading Links", *IEEE VTC '99*, pp. 300-304, 1999.
- <5>Richard van Nee, Ramjee Prasad, *OFDM for Wireless Multimedia Communications*, Artech House, 2000.
- <6>Kim, D. K., Do, S. H., Cho, H. B., Choi, H. J. and Kim, D. B., "A New Joint Algorithm of Symbol Timing Recovery and Sampling Clock Adjustment for OFDM Systems", *IEEE Transactions on Consumer Electronics*, vol. 44, No. 3, pp. 1142-1149, Aug. 1998.
- <7>Stefan H. Muller-Weinfurtner, "On the Optimality of Metrics for Coarse Frame Synchronization in OFDM: A Comparison", Personal, Indoor and Mobile Radio Comm., the 9th IEEE International Symp. on, vol. 2, pp. 533-537, 1998.
- <8>High-speed Physical Layer in the 5 GHz Band, IEEE Std 802.11a-1999.
- <9>Johansson, S., Landström, D. and Nilsson, P., "Silicon Realization of an OFDM Synchronization Algorithm", *IEEE*, pp. 319-322, 1999.
- <10>Daniel Landstrom, Sarah Kate Wilson, J.J. van de Beek, "Symbol time offset estimation in coherent OFDM systems" Comm., IEEE International conf. on, vol. 1, pp. 500-505, 1999.
- <11>Baoguo YANG, K. B. Letaief, Roger S. Cheng, Zhigang CAO, "Windowed DFT Based Pilot-Symbol-Aided Channel Estimation for OFDM Systems in Multipath Fading Channels", *IEEE VTC 51st*, vol. 2, pp. 1480-1484, 2000.
- <12>Gottfried Ungerboeck, "Channel Coding with Multilevel/Phase Signals", *IEEE Trans. on Inform. Theory*, vol. 28, no. 1, pp. 55-67, Jan. 1982.
- <13>Lou, H. L., "Implementing the Viterbi Algorithm", *IEEE Signal Processing Magazine*, pp. 42-52, Sep. 1995.
- <14>Wesel, Richard D. and Cioffi, John M., "Fundamentals of Coding for Broadcast OFDM", *IEEE Proceedings of ASILOMAT-29*, pp. 2-6, 1996.
- <15>Jonas Medbo, Henrik Hallenberg, Jan-Erik Berg, Propagation Characteristics at 5 GHz in Typical Radio-LAN Scenarios, IEEE, 1999